

## Ray and wave methods in complex geologic structures

Antonios P. Vafidis<sup>1</sup>, Ioannis F. Louis<sup>2</sup> and George A. Karantonis<sup>2</sup>

<sup>1</sup> Applied Geophysics Laboratory, Department of Mineral Resources, Technical University of Crete, Chania 73100, Greece

<sup>2</sup> Geophysics - Geothermy Division, Geology Department, University of Athens Panepistimiopolis Ilissia, Athens 15784, Greece

(Received 20 January 2001; accepted 4 July 2001)

---

**Abstract:** Seismic interpretation is usually checked by comparing field with synthetic data. A method for calculating synthetic data is chosen in terms of speed, efficiency and accuracy. In this study we compare three methods namely a 2D ray tracer for irregular grids, a finite difference method for travel time calculations and an acoustic wave propagation simulator. The comparison of calculated travel times is performed for a stratigraphic model and a salt model. The ray methods are fast and efficient by making certain approximations. The wave methods are more accurate but computationally more expensive.

---

**Key Words:** Seismic Modelling Methods, Ray-Tracing Simulators, Finite-Difference Propagators

---

### INTRODUCTION

The current practice of seismic data interpretation is usually based on trial and error forward modelling: synthetic travel times and/or synthetic seismograms are calculated for a particular model, and are compared against field records (Dai *et al.*, 1990). The model is modified until a reasonable match of theoretical and field times is achieved. This technique requires a practical and efficient method for calculating synthetic data. The interest in the extraction of fine detail from field seismograms has stimulated the search for numerical modelling procedures, which can produce synthetic seismograms for complex subsurface geometries and for arbitrary source to receiver separations.

The impressive improvement of the processing power and memory capability of modern computers made possible to implement inversion techniques (Phadke and Kanasewich, 1990). The inverse approach, as compared to trial and error interpretation has the advantage to provide quantitative estimates of the goodness of fit, the resolution and the no uniqueness of the solution. In addition, the time required for the interpretation is reduced and the best fitting solution is found by minimisation of a particular quantity according to a specific law, with no bias from the interpreter. In inversion algorithms the most time consuming step, in each iteration, is the solution of the forward problem. For this reason the development of fast and accurate modelling algorithms

is very important for the efficient application of the inversion method.

There are several options to compute the seismic response of a geologic model. In this study we carry out tests of three forward modelling algorithms based on ray and wave approximations. Comparison is based on speed, accuracy and efficiency for parallelism, factors that are essential for the implementation of the algorithms to an inversion code.

### THE ALGORITHMS

Asymptotic ray theory algorithms (Cerveny *et al.*, 1977, Zelt and Ellis, 1988) perform ray tracing for specified source-receiver pairs and calculate travel times and amplitudes along rays. On the other hand, the wave methods give a complete picture of the seismic wave field by accounting for the proper relative amplitudes of the various arrivals including the contribution of converted waves, diffractions from faulted zones and head waves.

Three seismic modelling codes are evaluated: The MINT2D, two point, 2D ray-tracing code (Vesnaver, 1996), the FAST2D finite difference technique (Vidale, 1988) and the ACO2D acoustic wave finite difference code (Vafidis *et al.*, 1992).

The MINT2D method, based on Fermat's principle of minimum time, computes the ray path by iterated perturbations of some initial guess on irregular grids. Fermat's principle is applied on three consecutive points where the ray intersects the pixel boundary. If

the initial and final points in a triplet are known the central is located in such a way that the travel time is minimum. Minimisation is carried for all triplets along the ray and is iterated until the sum of the ray point variations is smaller than a prefixed threshold or until a limit in the iteration number is reached. For example one can start from the source and the next two ray points, optimising the second point, then shift the attention to the second triplet (from second to fourth point) optimising the third and so on. The wave type of the ray path and its propagation geometry, called the “ray signature”, are input parameters.

The FAST2D method rapidly calculates the travel times of the first arriving seismic waves through any velocity structure. Wavefronts rather than the traditional rays are tracked. The timing process is initiated by assigning source point the travel time zero. The travel times of the points adjacent to source are then calculated. Next the travel times for the four corners are found by solving numerically the eikonal equation

$$\left(\frac{\partial t}{\partial x}\right)^2 + \left(\frac{\partial t}{\partial z}\right)^2 = s(x, z)^2 \quad (1)$$

where  $x, z$  are the space co-ordinates,  $t$  the time and  $s$  the slowness function. The travel times are found throughout the grid by performing calculations on rings of increasing radius around the source point.

ACO2D is a very efficient fast vectorized algorithm for seismic propagation with a finite difference scheme which is second order accurate in time and fourth order in space. Its formulation does not require numerical differentiation of the medium parameters. ACO2D describes acoustic wave propagation in a two dimensional heterogeneous medium. In order to calculate the earth response the equivalent first-order hyperbolic system of equations given below is solved numerically. This system consists of the basic equations of motion in the  $x$  and  $z$  directions, namely:

$$\rho(x, z) \frac{\partial}{\partial t} \dot{u}(x, z, t) = \frac{\partial}{\partial x} p(x, z, t) \quad (2)$$

$$\rho(x, z) \frac{\partial}{\partial t} \dot{w}(x, z, t) = \frac{\partial}{\partial z} p(x, z, t) \quad (3)$$

and the pressure-strain relation after taking the first time derivatives:

$$\frac{\partial}{\partial t} p(x, z, t) = K(x, z) \left[ \frac{\partial}{\partial z} \dot{w}(x, z, t) + \frac{\partial}{\partial x} \dot{u}(x, z, t) \right] \quad (4)$$

where the time derivatives of  $u(x, z, t)$  and  $w(x, z, t)$  represent the vertical and horizontal components of the particle velocity, respectively,  $p(x, z, t)$  denotes the pressure field, and  $K(x, z)$  is the bulk modulus. Equations (2) - (4) can be written in matrix form as

$$\frac{\partial}{\partial t} \begin{bmatrix} p \\ \dot{u} \\ \dot{w} \end{bmatrix} = \begin{bmatrix} 0 & K & 0 \\ 1/\rho & 0 & 0 \\ 0 & 0 & 0 \end{bmatrix} \frac{\partial}{\partial x} \begin{bmatrix} p \\ \dot{u} \\ \dot{w} \end{bmatrix} + \begin{bmatrix} 0 & 0 & K \\ 0 & 0 & 0 \\ 1/\rho & 0 & 0 \end{bmatrix} \frac{\partial}{\partial z} \begin{bmatrix} p \\ \dot{u} \\ \dot{w} \end{bmatrix} \quad (5)$$

or

$$\frac{\partial}{\partial t} U = A \frac{\partial}{\partial x} U + B \frac{\partial}{\partial z} U$$

which is a first-order hyperbolic system.

Dispersion analysis indicates that the shortest wavelength in the model needs to be sampled at six grid points/wavelength and the stability criterion is governed by

$$\ddot{A}_t < \frac{2}{3} \left( \frac{\ddot{A}_x}{V_{\max}} \right)$$

where  $V_{\max}$  is the maximum wave velocity,  $\ddot{A}_t$  is the time step and  $\ddot{A}_x$  is the grid digitisation interval. A spatially localised source is implemented by specifying the initial conditions applied to both particle velocity and pressure and using the source insertion principle of Alterman and Karal (1968). A buried line source is inserted having a Gaussian time excitation function.

## THE MODELS

For the needs of this study two different models are tested namely a salt and a stratigraphic model. Both models represent realistic geological structures with complex velocity distribution.

The test models were initially constructed in terms of constant velocity blocks, according to the requirements of MINT2D ray-tracing algorithm. Subsequent conversion of the constant velocity blocks to finite difference grids was performed for the needs of the algorithms FAST2D and ACO2D.

Accuracy of the model discretization depends on grid spacing. The grid spacing is kept less than the size of structures present in the model. In Fig. 1, we show minimum travel times calculated from FAST2D for a two layer model with a dipping interface and grid spacing 5 meters and 1 meter. For the denser grid the improvement in the accuracy is only 1% for receivers at distances larger than 30 m from the source.

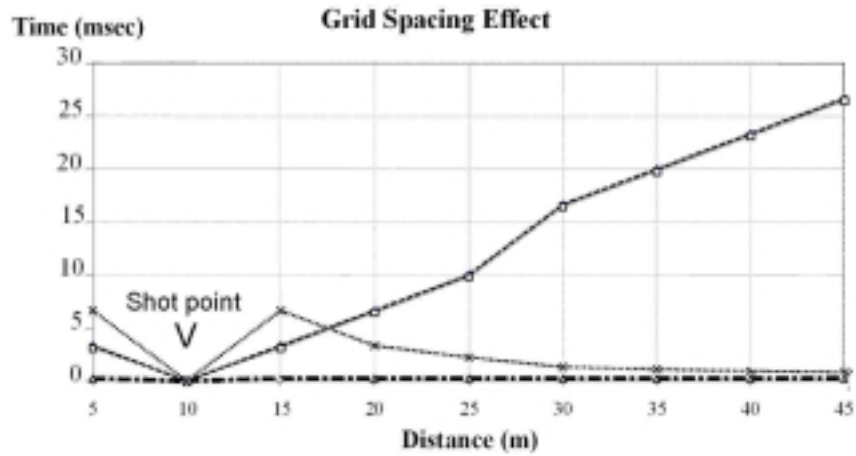


Fig. 1. Minimum travel times for a two layer model with a dipping interface and two different grid spacings.

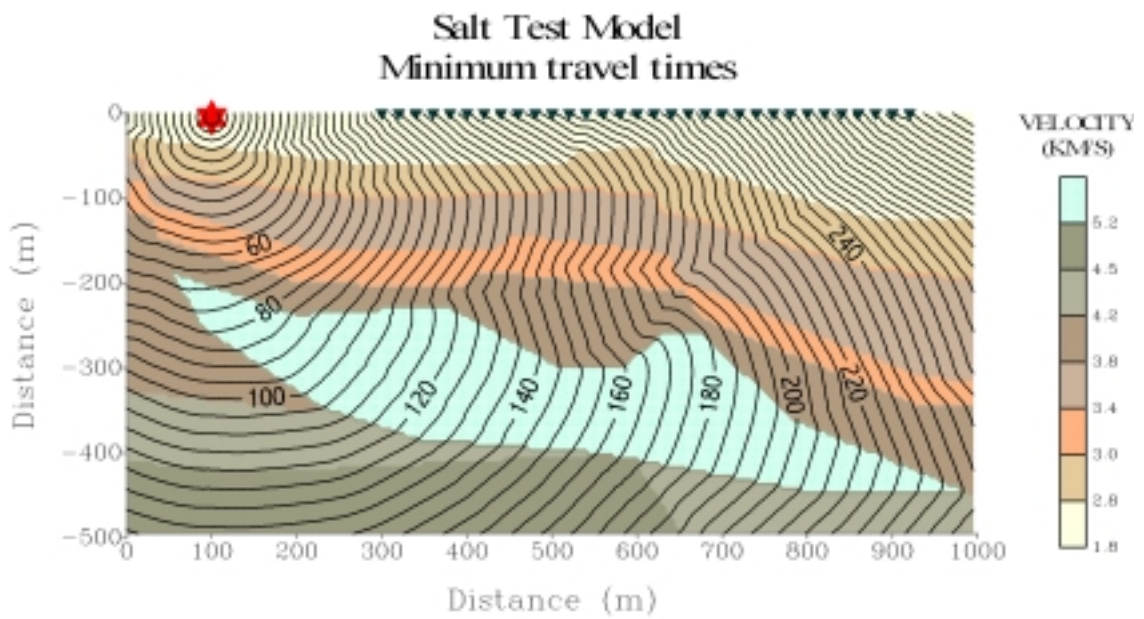


Fig. 2. The salt model and minimum time contours in msec calculated with the FAST2D algorithm.

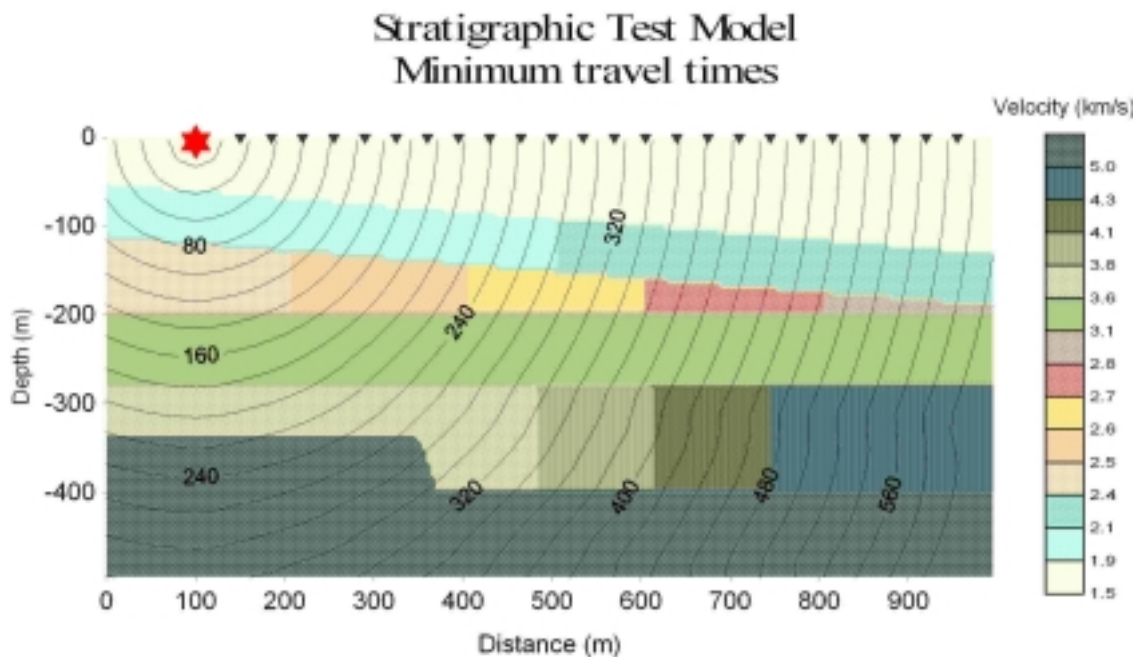


Fig. 3. The stratigraphic model and minimum time contours in msec calculated with the FAST2D algorithm.

Travel Time Curves for the Salt Model

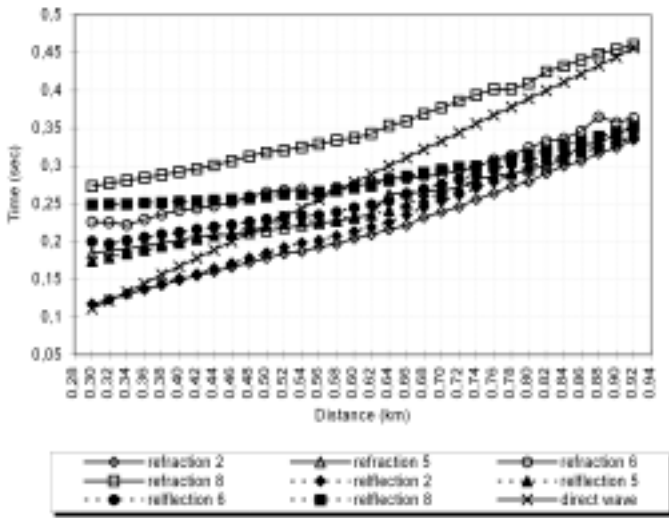


Fig. 4. Travel time curves of various seismic phases for the salt model calculated with the MINT 2D two point ray-tracer.

SYNTHETIC SEISMOGRAMS

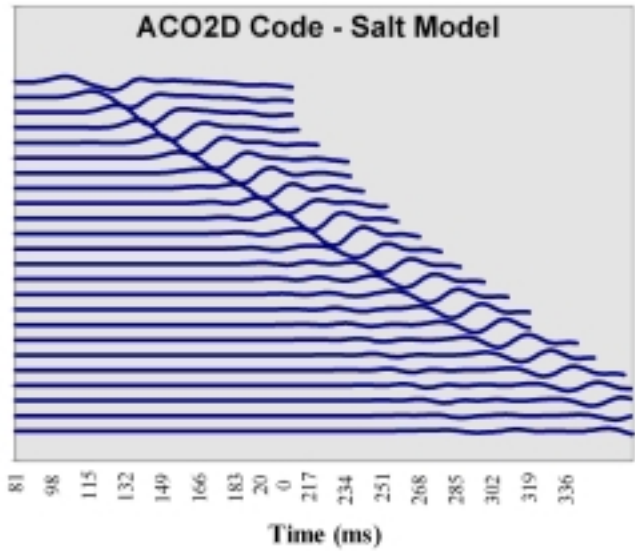


Fig. 5. Synthetic seismograms constructed with ACO2D algorithm. Source characteristics: Gaussian at 30 Hz.

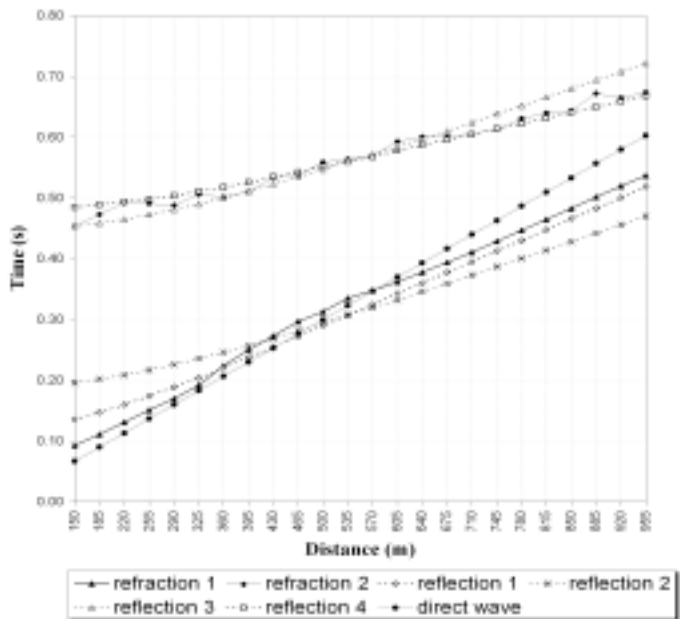


Fig. 6. Travel time curves of various seismic phases for the stratigraphic model calculated with MINT two point ray-tracer.

SYNTHETIC SEISMOGRAMS

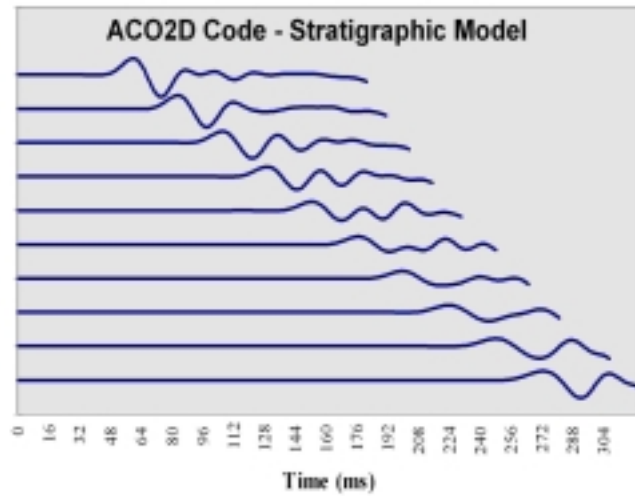


Fig. 7. Synthetic seismograms constructed with ACO2D algorithm. Source characteristics: Gaussian at 30 Hz.

**The salt model**

The salt model with an irregular interface geometry (Fig. 2) chosen for the evaluation of the algorithms is divided in constant velocity blocks. The size of the model is 1000 m by 500 m.

The number of nodes of the superimposed grid on the model utilised by the FD algorithms is 20.000 and the grid spacing is 5 meters. The number of geophones is 32. The geophones are placed at a depth of 5 m with the first geophone located 300 meters from the origin

of the model. The shot point is located 100 meters from the origin and the geophone spacing is 20 m.

**The stratigraphic model**

This model consists of six layers and a normal fault. The physical dimensions of the stratigraphic model (Fig. 3) are the same with the ones of the salt model. The source is placed at 100 m from the origin. A spread of 24 geophones with 35 m geophone spacing is used. Geophones are buried at a depth of 10 m and the first geophone is located at a distance 150 meters from the origin of the model.

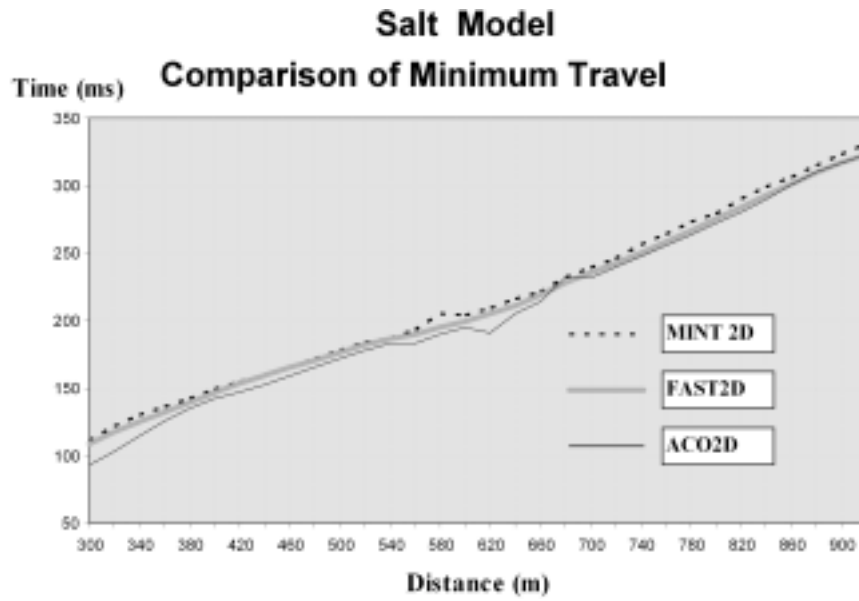


Fig. 8. Comparison of the minimum travel times, calculated by the three algorithms, for the salt model.

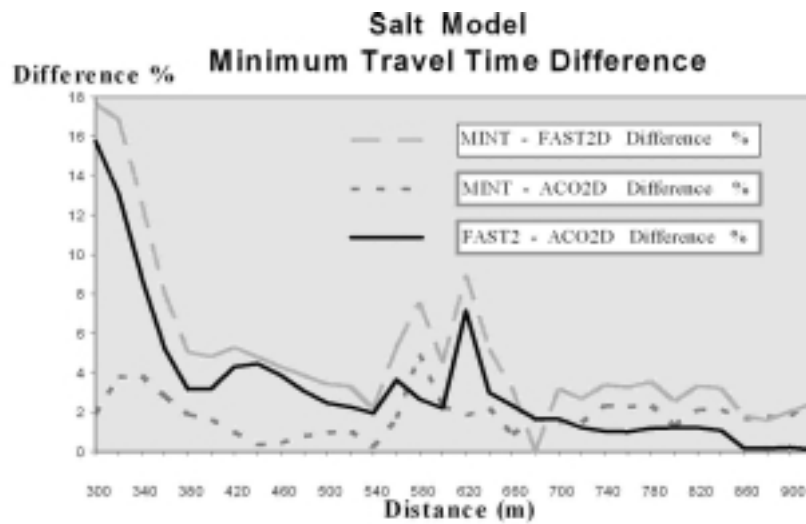


Fig. 9. Comparison of the travel time differences % for the salt model.

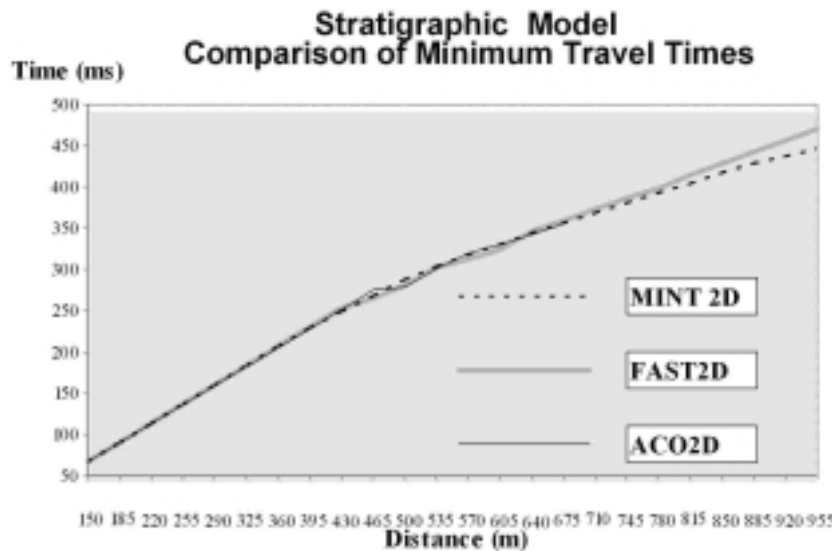


Fig. 10. Comparison of the minimum travel times, calculated by the three algorithms, for the stratigraphic model.

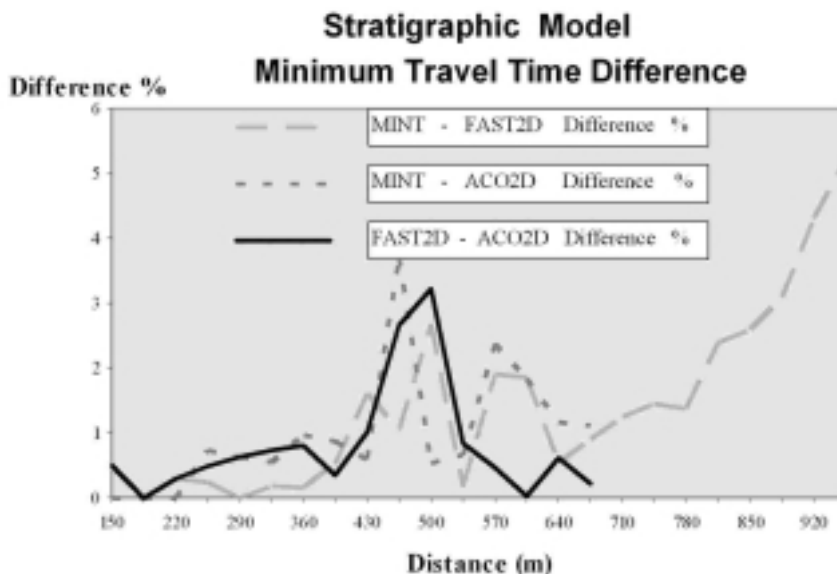


Fig. 11. Comparison of the travel time differences % for the stratigraphic model.

### The synthetic data

Synthetic seismic data are generated using the codes MINT2D, FAST2D and ACO2D.

### Salt Model Data

Travel time curves calculated from the MINT2D ray-tracer for various phases are shown in Fig. 4. The minimum time field obtained by the FAST2D is presented in Fig. 2. From the minimum travel times presented by contours, transmitted and refracted waves are identified. In Fig. 5 synthetic seismograms calculated from the ACO2D code are presented. For the construction of synthetic seismograms we utilised a Gaussian source wavelet with a dominant frequency of 30 Hz. Apart from the direct wave we clearly observe refracted waves for the distant geophones.

### Stratigraphic Model

Exactly the same calculations are made and the results are presented for this model in Fig. 3, 6 and 7. The synthetic seismograms are dominated by the high amplitude direct waves (Fig. 7). Head waves are not first arrivals for the geophone offsets involved in this simulation.

### Comparison of minimum travel times

The performance of the algorithms is evaluated by carrying out a comparison of the travel times of the first arrivals extracted from travel time curves, minimum travel time contour maps and synthetic seismograms.

Figures 8 and 9 present the calculated minimum travel times and their differences versus geophone

offset for the salt model. The maximum difference of about 18% is observed at small offsets. The smaller difference, almost systematically, is encountered between MINT2D and FAST2D codes. For the stratigraphic model (Figures 10 and 11) the travel time difference goes up to 4% at intermediate offsets. The difference in minimum travel times calculated from MINT and FAST2D at large offsets shows a linear dependence on offset.

## EFFICIENCY OF PARALLEL IMPLEMENTATION

MINT2D ray-tracer and FAST2D Finite Difference propagator have been implemented for parallel computation and have been evaluated for their efficiency by Kofakis and Louis (1995) and Louis *et al.* (1996). They have presented a very cost-effective efficient solution for the parallel implementation of these algorithms in a network of workstations using the Parallel Virtual machine (PVM) platform.

Several tests of the parallel implementation of the MINT2D ray-tracing algorithm were performed using a data set consisting of 4 sources and 48 receivers. The tests were done on a cluster of SUN workstations all with zero load (no user tasks other than the slave processes running). Fig. 12 is a graph of the time spent by the computer for input of parameters (set-up time); calculations time; the time from the moment the computer sends the tasks to the slaves till it has collected and synthesised the results overall the slaves (collection time); the time of a single process (one slave) divided by the number of slaves (ideal time) and the total elapsed time (the sum of set-up, calculations and collection times).

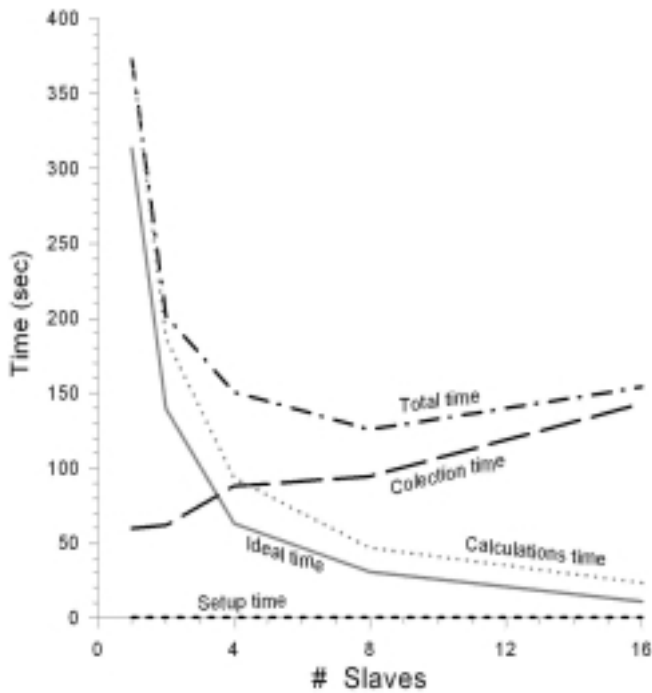


**Fig. 12.** Diagram of the time spent by the computer for input of parameters (set-up time); calculations time; the time from the moment the computer sends the tasks to the slaves till it has collected and synthesised the results overall the slaves (collection time); the time of a single process (one slave) divided by the number of slaves (ideal time) and the total elapsed time (the sum of set-up, calculations and collection times) for 125 rays and different number of processors (slaves).

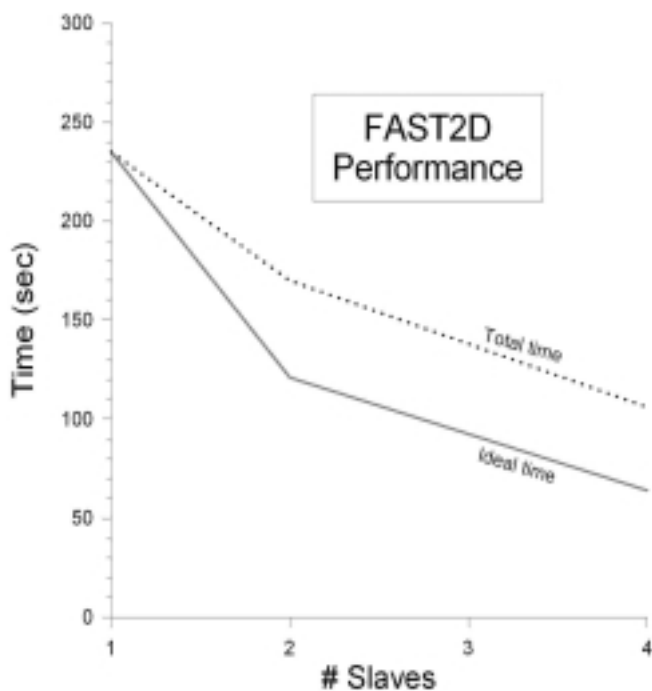


**Fig. 13.** Diagram of elapsed times.

Although there is a significant speed-up in the execution and calculation part, a considerable time is also spent for the collection of the results. This time is mainly spent by the master processor because the file input/output is performed by the master in a serial way (via NFS). The initial set-up and initialisation time is not significant and is slightly improved when a slave is called many times by the master since initialisation is performed only once. MINT2D algorithm has therefore a strong parallel decomposition aspect and therefore it is particularly suited for parallel implementation.

FAST2D code cannot be implemented on vector or parallel computers in the same way as the MINT ray-tracer because it is sequential in the sense that in order to compute the travel times for a box, the travel times of the inner box have to be calculated in advance. It is however susceptible in a kind of parallelism where the grid of nodes is decomposed and distributed among the processors (*domain decomposition*). For FAST2D propagator it was adopted the *model distribution* technique where the grid of nodes constituting the model is decomposed into parts and assign the parts to different processors.

Several tests for the efficiency of FAST2D finite-difference code for parallel implementation were performed using a source located in the centre of a 1000x1000 grid. The tests were done on a cluster of SUN workstations all with zero load. The graph of the elapsed times for the total and ideal times is given in Fig. 13. The drawback in this case is that the best allocation of processes on processors must be known before execution (in advance) and not in runtime (*static load balancing*).

ACO2D is written in a way ensuring its efficiency for implementation on vector computers (Vafidis *et al.*, 1992). This is achieved by expressing the numerical operations in vector form and performing matrix multiplication by diagonals. This technique increases the computational speed 30-100 percent versus the non-vectorised code.

## CONCLUSIONS

The comparisons of the modelling algorithms for complex geologic models suggest that these methods are compatible in terms of the accuracy of the travel times. Further accuracy tests are necessary by comparing the numerical solutions with analytic solutions.

- FAST2D propagator is an easy to use and relatively fast algorithm calculating first arrival times. It models only the kinematic properties of the wave equation and it works satisfactory in complex models

with smooth velocity contrasts. Its sequential scheme makes it not easily converted to parallel implementation.

- MINT2D two point ray-tracer works also very satisfactory in relatively complex models, and arrival times for various seismic waves are calculated. Calculation of arrival times for more seismic phases is very useful in the interpretation. It has a strong parallel decomposition aspect making it ideal for parallel implementation.

- ACO2D algorithm is full waveform Finite Difference propagator. It models the kinematic and dynamic properties of the seismic waves and produces synthetic seismograms, which can be extremely useful in the interpretation procedure, when compared with the actual field seismograms. Its structure is ideal for implementation on vector computers.

### ACKNOWLEDGEMENTS

The research leading to this article was funded by the EU Research Project “3D Asymptotic Seismic Imaging”, Contract JOU2-CT93-0321.

### REFERENCES

Alterman, Z.S. and Karal, F.C., 1968. Propagation of elastic waves in layered media by finite difference methods. *Bull. Seis. Soc. Am.*, **29**: 367-398.

- Cerveny, V., Molotkov, I.A. and Psencik, I., 1977. *Ray method in seismology*, The University of Karlova, Praha.
- Dai, N., Vafidis, A. and Kanasevich, E.R., 1990. Surface seismic simulations in steam injection EOR problems with finite differences. *AOSTRA Journal of Research*, **6**: 199-210.
- Kofakis, G. P. and Louis, F.I. 1995. Distributed parallel implementation of seismic algorithms. In *Mathematical Methods in Geophysical Imaging III*, Siamak Hassanzadeh, Editor, *Proc. SPIE 2571*, 229-238, San Diego, California.
- Louis, F.I., Kofakis, P. and Karantonis, G. 1996. Parallel Implementation of seismic modelling algorithms based on ray and wave methods. *Final Report submitted to EU within the frameworks of JOULE II Project*, Athens.
- Phadke, S. and Kanasevich, E.R., 1990. Seismic tomography to obtain velocity gradients and 3D structure and its application to reflection data on Vancouver island. *Jour. of Earth Sci.*, **27**: 104-116.
- Vafidis, A., Abramovici, F. and Kanasevich, E. R., 1992. Elastic Wave Propagation Using Fully Victories High Order Finite Difference Algorithms. *Geophysics*, **57**: 218-232.
- Vesnaver, A. L., 1996. The contribution of reflected, refracted and transmitted waves to seismic tomography: a tutorial. *First Break*, **14**: 159-168.
- Vidale, J. E., 1988. Finite difference calculations of travel times. *Bull. Seis. Soc. Am.*, **78**: 2062-2076.
- Zelt, C.A. and Smith, R.B., 1992. Seismic travel time inversion for 2-D crustal velocity structure. *Geophys. J. Int.*, **108**: 16-34.